Electronic Supplementary Material (ESI) for Nanoscale.


# Nanomechanical Sandwich Assay for Multiple Cancer Biomarkers in Breast Cancer Cell-derived Exosomes

*Hashem Etayash, Ryan McGee, Kamaljit Kaur and Thomas Thundat*

**This file contains:**

**S1. Complementary introduction:**

One crucial key to achieve an effective treatment of cancer is by diagnosing the condition fast (i.e., in earlier stages of its development). Earlier detection of cancer can lead to more treatment options and a better chance of survival[1]. Unfortunately, in its early stages, breast cancer has no symptoms and is difficult to identify. Therefore, there is an urgent need for a new discovery of specific markers and effective tools that can allow fast screening and diagnosis of the disease[1].

Exosomes (nanoscale vesicles) that shed from tumor cells into the peripheral blood circulation have recently attracted substantial attention as alternative biomarkers to recognize cancer earlier before it spreads[2, 3]. These vesicles range in diameter from 30 nm to 100 nm, carrying valuable information about their parental tumors and hold proteomic and genetic information identical to that present in their original cells. Simple blood tests to detect those exosomes in biofluids of cancer patients would be complement to other approaches of disease diagnosis and treatment monitoring. Unlike circulating tumor cells (CTCs) and other cancer biomarkers, exosomes can be found in most biofluids of the body including; blood circulation, urine, saliva, breast milk, ascitic and amniotic fluids. Exosomes also exist in much higher concentrations than CTCs. CTCs exist in the bloodstream in small numbers[4], around 1 to 100 cells per mL, exosomes concentration can be between $10^9$ to $10^{11}$ exosomes per mL in plasma. Exosomes are particularly interesting as cancer biological markers because they are stable carriers of genetic materials and proteins from their original cells. They are part of the disease process, for example; tumor angiogenesis, metastasis, cell communications and growth[5]. Such as CTCs, exosomes contain diverse types of membrane proteins that can be targeted for selective detection. Tumor cells were recently found to shed tens of thousands of exosomes daily into the blood circulation at earlier

and late stages that carry their specific signatures. These exosomes thus, hold potential as biomarkers to identify the disease earlier and to further study other ambiguous properties of cancer.

Unfortunately, the technical challenges and limitations of the current techniques in isolating and detecting exosomes have hindered the clinical use of those nanoparticles as biomarkers in cancer field to improve patient care[6]. In this study, we report the use of a microcantilever array sensor for detecting breast cancer cell exosomes at ultra-low concentrations. We compare the approach to currently available methods and we show a new form of nanomechanical sandwich assay to achieve an extraordinary detection limit. The study also raises the support to use glypican-1 as a breast cancer biomarker to identify the disease early.

**S2. Microcantilever array and the Principle of Operation:**

A microcantilever is a nanoscale sensing device that measures surface stress and nanomechanical distance in a form of cantilever's bending or/ deflection (nm). Microcantilever sensors have gained a great deal of attention in last few decades for its ability to detect changes in temperature, pressure, relative humidity and detect binding of extraordinary small numbers of chemical and biological analytes with high sensitivity[7]. The microcantilever resembles a miniature diving board that can be easily fabricated on silicon wafers or other materials using conventional microfabrication techniques. In most biomedical applications, the microcantilever beam is functionalized with specific ligands in order to capture the targeted analytes. During the operation, the immobilized ligands selectively capture the target in the solution from the surrounding medium, resulting in cantilever's bending (deflection in nm)[7, 8]. This also can be

read as a change in the resonance frequency; however, since liquids can heavily damp the resonance frequency, this measurement technique is not routinely used in liquid sensing. The adsorption-induced cantilever deflection is largely independent on the medium; thus, it is regularly used as a sensing method. The detection specificity relies deeply on the molecular interaction between the immobilized ligand and the target.

## S3. Drawbacks of the Current Exosomes Detection Techniques and Advantages of Microcantilever Array

Despite their potential use as cancer biomarkers, exosomes can be very challenging to detect in biofluids due to a number of factors. First, exosomes have very small size (nanoscale range), which make their detection with simple instrumentation impossible. Similarities of cancer cell-derived exosomes to those exosomes from normal epithelial and haematological cells make it difficult even using the current techniques to accurately isolate them[9, 10]. Conventional separation techniques like ultracentrifugation and the density-gradient method separate exosomes based on their size and buoyant density[6], making it impossible to separate cancer cell-derived exosomes from noncancerous-derived exosomes as they may have the same densities. Techniques such as enzyme-linked immunosorbent assay (ELISA) and western blot analysis are more sensitive and specific; however, they require large amounts of samples and extensive labeling[11]. In addition, they are very expensive and require highly trained technicians. The commercially available Nanoparticle Tracking Analysis (NTA) and Dynamic Light Scattering (DLS) techniques are currently the ideal tools to sort nanoparticles in the size range of 10 nm – 2 $\mu$m. Nevertheless, they can only be useful to detect high concentrations of nanoparticles ($10^6$ to $10^9$ particles $mL^{-1}$)[6, 12]. Flow cytometry has come with a few advantages over other techniques as it can allow individual exosomes to be resolved and allow the surface-markers to be measured per exosome[13]. However, the main drawback of the system is its recovery signals that do not allow the system to

resolve nanoparticles less than 300 nm in size. State-of-the art microscopy, such as the transmission electron microscopy (TEM) and the scanning electron microscopy (SEM) are very powerful tools in studying small size particles; they are very complementary to the above mentioned techniques as they can provide size, concentrations and morphological structure of exosomes with 0.1 nm sizes and above[14]. However, the main disadvantages beside their cost, is their lack of specificity (i.e., they can't discriminate tumor-derived exosomes from no tumor-derived exosomes).

The use of miniature sensors, such as microcantilevers, for rapid detection are increasingly finding applications in many different fields including; chemical analysis, drug discovery, blood analysis, treatment monitoring, microbial detection, food/water analysis, and in point-of-care medical diagnostics[7]. The microcantilever is a high throughput platform that can detect a myriad of chemical and biological analytes in real-time with extreme sensitivity[15]. Besides being a label-free detection device, microcantilevers are extremely sensitive, reliable, scalable and simple to use. Microcantilevers have the capability to detect biomolecules in liquid at nano to femtomolar concentrations[16, 17]. The microcantilever has been widely used in numerous applications to detect several chemical and biological entities including nucleotides,[18-23] proteins,[24] microorganisms[25-28] a wide range of toxic chemicals[29-34] and most recently in cancer biomarkers and gene transmutations.[35-37] In addition, when microcantilevers are operated in a vacuum they have demonstrated zeptogram mass resolution.[38]

In comparison to the above mentioned methods, the microcantilever array can provide very selective and sensitive detection of tumorigenic exosomes by attaching specific receptors on it. The detection limit is far superior to what is been reported on the above techniques. The system is very simple, inexpensive and applicable for multiplexing detection with real-time monitoring.

Using a mechanical sandwich assay in our study has further enhanced the sensitivity of the detection by orders of magnitudes.

**S4. Methods:**

**Probes for Targeting Exosomes.** The following monoclonal antibodies were used without any further modification; antiCD24 (Abcam, clone eBioSN3), antiCD63 (Abcam, clone SPM110), antiGPC1 antibody (EMD Millipore, clone 4D1) and antiEGFR antibody (Abcam, clone EGFR.1).

**Microcantilever Arrays Preparation.** Microcantilever arrays with eight gold-coated microcantilevers (Concentris GmbH – Switzerland), 1000 μm long, 100 μm wide and 1 μm thick, were used in the experiments. The top surfaces of the cantilevers (20 nm gold thickness) were functionalized individually with the above designated monoclonal antibodies, following a previously described protocol[39]. Initially, the arrays were cleaned with Piranha solution (3:1 by volume 96%H2SO4:30%H2O2) for 15 minutes, rinsed with MilliQ-water (18 MW), ethanol and dried in air. The arrays were then incubated in 2[methoxy (polyethyleneoxy) propyl] trimethoxysilane (10 mM, Gelest Inc. Frankfurt, Germany) for 20 minutes in order to render the backside of the levers inert to interactions. The cantilevers were then rinsed again with ethanol and dried in air. In order to immobilize the antibodies, the arrays were first coated with a thiolated linker ($HSCH_2CH_2NH_2$) by treating the surface with a cysteamine hydrochloride (0.01 M) in a concentrated buffer solution (8× PBS, pH 8.1) for 6 h. The arrays were then rinsed with 1× PBS (pH 7.4) to remove any unbound cysteamine. The accessible carboxylic terminal of monoclonal antibodies (at a concentration of 50 μL $mL^{-1}$) was activated by NHS/DCE (solution of 0.10 M NHS and 0.4 M EDC in deionized water) for 10 min and allowed to interact with the

free amine groups of the pre-attached cysteamine linker. *Note*: functionalization of the two self-assembled monolayers (cysteamine and the mAbs) was performed using the capillary coating apparatus (Concentris – Switzerland) in order to differentially functionalize each cantilever in the array with different antibodies. Prior to use the array was rinsed with 70% ethanol and copious amounts of PBS solution to remove any physically adsorbed materials.

**Cell Lines**. Human breast cancer cell lines (MDA-MB-231, MCF7) and human mammary epithelial cell line MCF-10A (American Type Culture Collection, Manassas, VA) were used in the experiments. The first two were cultured in a DMEM medium containing 10% exosomes-depleted fetal bovine serum (FBS), 100 IU $mL^{-1}$ penicillin, and 100 IU $mL^{-1}$ streptomycin. MCF10A however, was cultured in minimal essential growth medium (MEGM, Lonza, Cedarlane) supplemented with the same additives as mentioned above. All cell lines were incubated at 37 °C in a 5% $CO_2$–95% $O_2$ incubator and the growth media were replaced every 48 h.

**Exosomes Isolation from Cell Lines**. When cells reached confluence, the media was collected and centrifuged at 800g for 5 min, followed by a centrifugation step of 2,000g for 10 min to discard dead cells and cellular debris. The supernatant was filtered through a 0.2 μm pore syringe filter (ROSE Scientific Ltd, CA). The collected media was then ultra-centrifuged at 100,000g for 2 h at 4 ºC and exosomes pellet was subjected to a PBS washing steps followed by another ultra-centrifugation at 100,000g for 2 h at 4 ºC. While the supernatant was discarded, the exosomes pellet was suspended in 500 μl of sterile PBS. Frothy microliters of these exosomes were used for DLS analysis after dilution in PBS for independent measurement of exosomes concentrations.

**Concentration of Exosomes Proteins**. The proteins concentration (surface proteins) of the exosomes was determined using Bradford Protein Assay (Bio-Rad, Hercules, CA) with bovine serum albumin (BSA) as a standard. Procedures were carried out according to the manufacturer's instructions.

**Dynamic Light Scattering (DLS).** Exosomes size distribution and concentrations determined via DLS was carried out using a Zetasizer nanoseries instrument (Malvern Nano-Zetasizer, 633 nm He- Ne laser (4 mW)), operating at a 173° angle. Samples (~ 0.5 mg $ml^{-1}$ total protein concentration as measured by Bradford assay) were placed in solvent-resistant micro cuvettes at 40 µL and measured for light scattering at a fixed position with an automatic attenuator. The temperature was controlled at 25C°. The presented data is an average of five replicates. The extracellular vesicles (exosomes) intensity distributions P1(r) are presented in **supplementary Fig. 1**. According to previous studies,[18] when the area of P1(r) is aligned to the Rayleigh Ratio R(q), the integral of the number-weighted radius distribution PN(r), represents the number of exosomes per mL (**see supplementary Fig. 1e**). The refractive index of exosomes is currently unknown; therefore, it's imported from another reference[40] as 1.46. The size distribution of the purified exosomes, determined by DLS, was found between 86 nm to 112 nm (**supplementary Fig. 1a, b, c, d**), which is in a good agreement with data, published elsewhere[2, 41]. Moreover, three different concentrations of exosomes were perceived, $6.13 \times 10^{12}$, $5.1 \times 10^{12}$, and $4.3 \times 10^{12}$ exosomes $mL^{-1}$, for MDA-MB231, MCF7 and MCF10A, respectively. Next, we adjusted the sample concentration by comparing the data from DLS to the Bradford protein concentration assay (**supplementary Fig. 2b**) and performed serial dilutions afterward, for the cantilever experiments.

**Scanning electron microscopy (SEM)**. All samples were fixed with 3.7% glutaraldehyde (Sigma–Aldrich) in phosphate buffered saline for 10 min, washed twice with PBS and dehydrated with ethanol. The samples were then left to dry at room temperature for several hours on a silicon substrate and then analyzed by scanning electron microscopy with a 5keV accelerating voltage (Sigma FE-SEM, Carl Zeiss) after gold sputtering. **Supplementary Fig. 2a** shows selected SEM images of exosomes from the three different cell lines; MDA-MB231, MCF7 and MCF10A.

**Microcantilever Measurements and Data Analysis**. The cantilever experiments were carried out using a home-made microcantilever setup was previously described[8]. Prior to running the exosomes, the functionalized microcantilever array placed in the fluidic cell was equilibrated by running a solution of phosphate buffered saline (PBS): human serum solution (1:1 vol/vol) at a constant flow rate of 1 mL $h^{-1}$ until a stable baseline was achieved (serum was diluted in PBS and filtered through a 0.2 μm pore-filter prior the use). The microcantilever array was then exposed to a running PBS/serum solution for approximately 50 scans followed by flow of a solution containing cancer cell exosomes. The experiments were performed for three different isolated exosomes (from MDA-MB231, MCF7 and MCF10A) and several different concentrations as indicated in the text (from $10^{-6}$ g $mL^{-1}$ to $10^{-15}$ g $mL^{-1}$). After exosome injection, the microcantilever array was washed with PBS for 10 minutes at the same flow rate. For running the microcantilever assay and performing the capture efficiency experiments, mixed concentrations of exosomes from cancer cell line (MDA-MB231) and non-cancerous cells (MCF10A) were prepared with up to 20-fold excess of MCF10A-derived exosomes (**supplementary Fig. 3**). The final concentration was fixed at 1 μg $mL^{-1}$. Samples were then injected individually into the cantilever sensor and the data was recorded in real-time. Further

control experiments were performed by injecting two samples, contained an exosomal bound antigen GPC1 at 1 μg $mL^{-1}$ or samples free from antigens for control, in order to evaluate cantilever's response to the exosomes antigens. All data from nanomechanical cantilever deflections was recorded in real-time using a multifunctional data-acquisition board driven by LabVIEW-based software.

**Antibody Conjugation to Gold Nanoparticles**. Spherical gold nanoparticles (diameter = 100 nm) were purchased from Nanopartz™. The mAb-coated Au nanoparticles (NPs) were prepared according to the previously described immobilization technique. Briefly, 100 μL of 1 mg $mL^{-1}$ Au NPs in PBS were mixed with 100 μL of 1 mg $mL^{-1}$ cysteamine hydrochloride in PBS (8× PBS, pH 8.1) and incubated for 6 h at room temperature. 500 μL of 1% poly (ethylene glycol) (MW 20 000; Sigma) was then added to the mixture to prevent aggregation and the solution was centrifuged at 6000 rpm for 30 min. The supernatant was removed and the pellet (cysteamine-coated gold NPs) was redispersed in a 100 μL PBS solution (pH 7.4). 50 μL of antiGPC1 mAb was added to 450 μL PBS, containing 100 μL of carboxylic group activating agent (solution of 0.10 M NHS and 0.4M EDC in deionized water, prepared separately, then added to the mAb solution). The mAb solution was left for 10 min for activation before incubation with cysteamine-coated NPs for 12 h at room temperature. As previously proven[39], the accessible carboxylic terminal of mAb will be activated to interact with the free amine groups of the pre-attached cysteamine linker. The solutions were completed to 1 mL with PBS, 500 μL 1% poly (ethylene glycol) was again added to prevent aggregation and centrifuged at 6000 rpm for 30 min. The supernatant was removed and the pellet (antiGPC1-coated gold NPs) was redispersed in a 1 mL PBS solution (pH 7.4) and stored at $4^0$C until its use.

**Exosomes Detection in a Nanomechanical Sandwich Assay.** The microcantilever array functionalized with antiGPC1 mAb was first equilibrated by flowing a solution of phosphate buffered saline (PBS): human serum solution (1:1 vol/vol) at a constant flow rate of 1 mL $h^{-1}$ until a stable baseline was generated (note that the serum was diluted in PBS and filtered through a 0.2 μm pore filter prior its use). Following this, the cantilever array was subjected to 1 mL PBS/serum solution containing exosomes derived from cancer cell MDA-MB231 or normal cells MCF10A, at concentrations ranging from $10^{-9}$ g $mL^{-1}$ to $10^{-15}$ g $mL^{-1}$ (**See supplementary Fig. 4**). To amplify the cantilevers signal, a $2 \times 10^{-12}$ g $mL^{-1}$ solution of antiGPC1-coated nanoparticles (~ 500 NPs) was injected into the system and allowed to incubate for 1 hour before an ultimate wash with PBS solution. Note: the concentration of the antiGPC1-coated NPs was adjusted after several optimization experiments (**supplementary Fig. 5**). Different concentrations of antiGPC1-coated NPs ($10^{-6}$ to $10^{-12}$ g $mL^{-1}$) were introduced into the sensor following the injection of fixed concentration of exosomes ($10^{-13}$ g $mL^{-1}$, ~ 200 exosomes $mL^{-1}$). From the results it can be seen that the noise from the NPs is a minimum at $2 \times 10^{-12}$ g $mL^{-1}$, which correspondingly represents the lowest noise ratio. The result is illustrated in the **supplementary Fig. 5** with averaged values of three replicates. A similar experiment was performed with control cantilevers, as indicated, for comparison. Data from nanomechanical cantilever deflections were recorded in real-time using a multifunctional data-acquisition board driven by LabVIEW-based software. Each experiment was repeated three times and the averaged values, mean ± s.d., were presented.

**Statistical analysis**. The statistical analyses were carried out using either, the unpaired student's t-test or the one-way ANOVA as specified elsewhere. All experiments were performed as a minimum of three independent repeats and the signals of identically functionalized cantilevers

were averaged. P-values of less than 0.05 were considered statistically significant. Data is presented as mean ± s.d. throughout the manuscript.

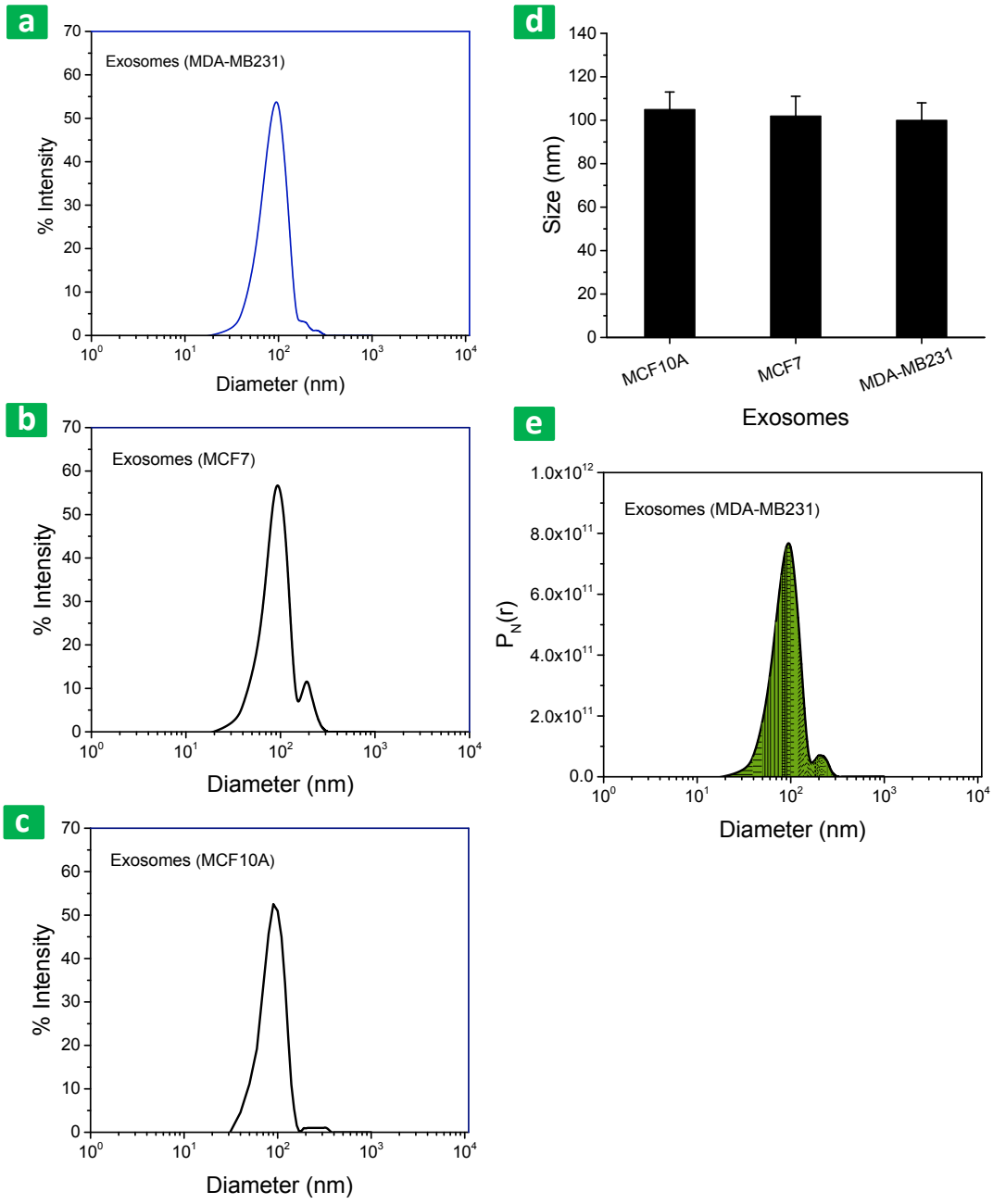


**Fig 1.** Dynamic Light Scattering (DLS) determines the absolute exosomes size distribution for the tested cell lines as indicated in spectra **a, b** and **c**. An averaged size determined by DLS is

presented in figure **d**. The difference from SEM (~89 ±5 nm) compared to Dynamic Light Scattering (around ~102 ±8 nm) is due to the fact that the DLS monitors the hydrodynamic diameter of the exosomes in solution. In addition, larger particles contribute more strongly to the light scattering than the smaller particles which cause more shifts in the distribution values. Values of an average calculation of three replicated is presented with ± s.d. **e.** Concentration of exosomes (vesicles per mL) as it recovered from the vesicles' distribution, $P_N(r)$ represents the number of vesicles per mL.

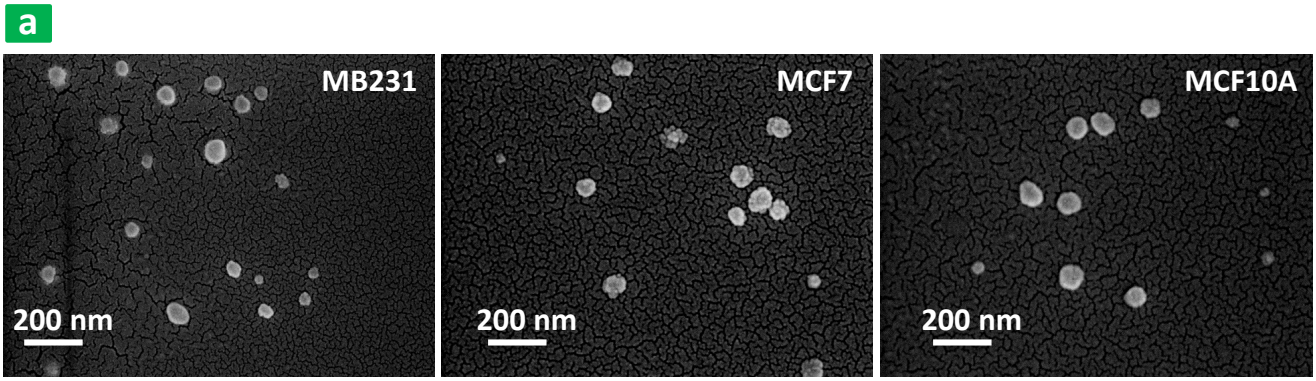


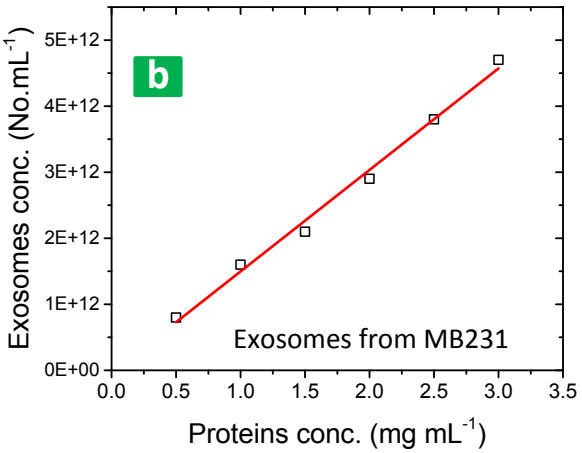


**Fig 2**. Scanning Electron Microscopy (SEM) images of exosomes produced breast cell lines as indicated, MB231, MCF7 (cancerous cells) and MCF10A (noncancerous cells). The result shows comparable exosomal distribution with an average size value of ~89 ±5 nm in all experiments. Figure **b** represents a linear correlation between quantification of exosomal proteins measured by Bradford assay (mg per mL) and concentration of the exosomes (number per mL) measured by Dynamic Light Scattering. The plot indicates a linear relationship between the vesicles number

and protein concentration. An average of three replicate measurements is presented.

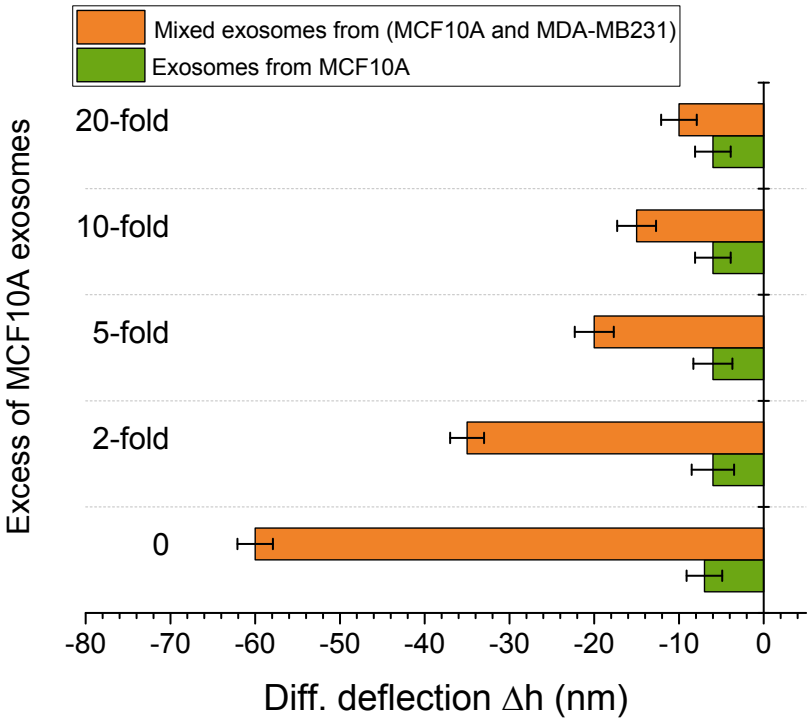


**Fig 3.** Differential nanomechanical deflection (Δh) measured after injection of different ratios of exosomes from cancer cells (MDAA-MB231) and noncancerous exosomes from MCF10A cell line. The results indicate significant deflection in presence of cancer cell-derived exosomes in comparison to the reference (exosomes only from MCF10A). The results indicate that the antiGPC1-functionalized cantilever can still detect cancer cell-derived exosomes in the presence of a 20-fold excess of non-cancerous exosomes. Mean values are presented with error bars indicating s.d.

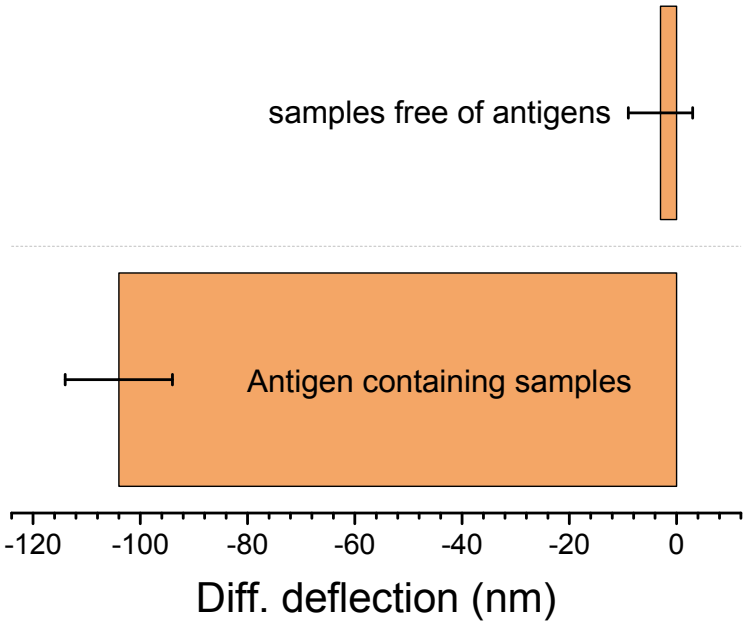


**Fig 4**. Experiments show differential nanomechanical deflection (Δh) of the cantilevers coated with antiGPC1 mAb after exposure to two samples, as indicated. The first sample contains the exosomal bound antigen GPC1 and the second is free of antigens. i.e., 1 ml of sterile-buffer/human serum sample of 1:1 v/v, contains 1 µg $mL^{-1}$ the exosomal bound antigen GPC1, or free of antigens. The cantilever demonstrates significant differential deflection in presence of exosomes bound antigen compared to the second sample. The results indicate the specific response of antiGPC1-functionalized cantilever to the corresponding exosomal bound antigen and provide further support to the behaviour of the cantilever towards exosomes surface antigens. The study is presented as mean ± s.d. values of three replicates.

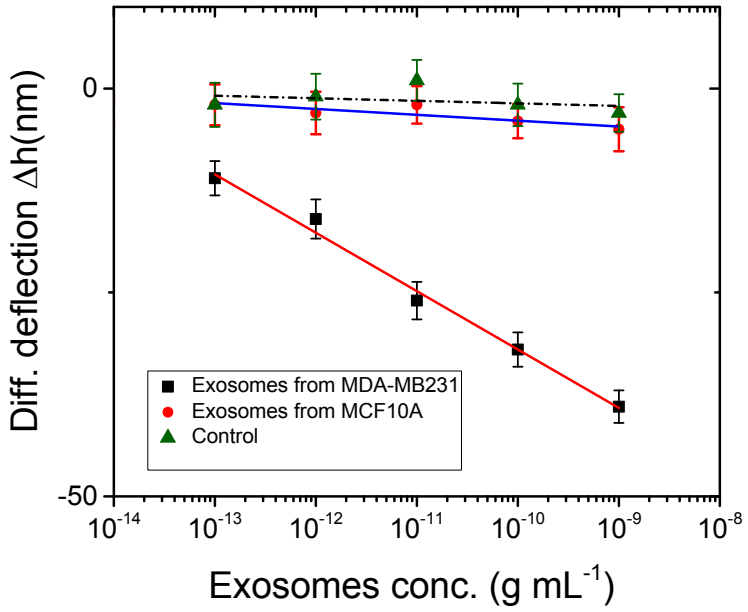


**Fig 5**. Exosomes concentration as a function of fixed antiGPC1-coated NPs. Enhanced nanomechanical bending (nm) is scaled proportionally with the exosomes concentration in the samples. The plot shows a limit of detection of $10^{-13}$ g $mL^{-1}$ at which the cantilever signal is statistically significant from those observed with normal cells-derived exosomes and the reference control. The control signal is a microcantilever-coated with only cysteamine, exposed to exosomes at the same concentrations as indicated, then exposed to antiGPC1-coated NPs at fixed concentration ($2 \times 10^{-12}$ g $mL^{-1}$). Values represent an average calculation of three replicates and error bars indicate s.d.

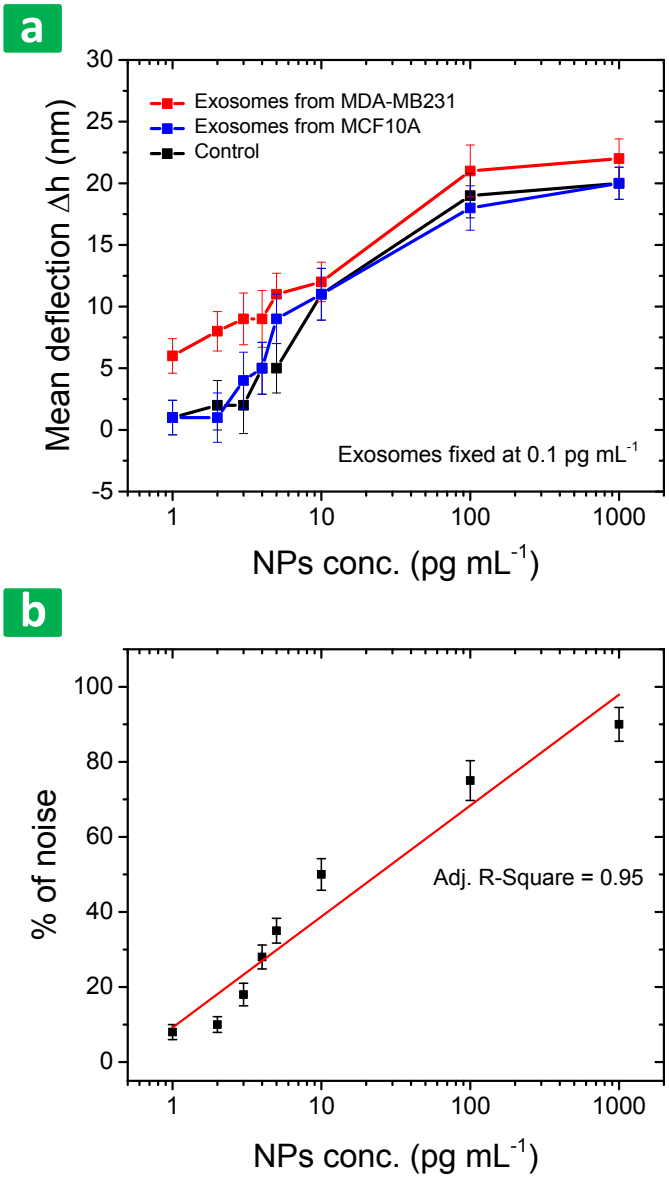


**Fig 6.** Microcantilever sandwich assay, nanomechanical deflection (nm) as a function of concentration of antiGPC1-coated nanoparticles (NPs). **a.** Deflection of the cantilever due to exposure to different concentrations of NPs at fixed concentration of exosomes ($1 \times 10^{-13}$ or o.1 pg $mL^{-1}$). Results represent mean ± s.d. of three replicates. **b.** The noise ratio of the cantilever increases as a function of the number of NPs at the tested exosomes level (0.1 pg $mL^{-1}$). In other words, the generated signals of the cantilever become less significant by increasing the number of functionalized NPs, indicating a saturation point at $2 \times 10^{-12}$ g $mL^{-1}$ or/ 2 pg $mL^{-1}$ NPs concentration (maximum significance and minimum noise). The results suggest that the

maximum number of antiGPC1-coated NPs on the surface is ~400 for exosomes concentration 200, based on the calculated mass and number of NPs provided by the manufacturer. This agrees well with our geometrical calculation that estimates number of NPs on the surface to ~500. This leads us to suggest also that the enhanced cantilever surface stress may be due to NPs binding to more than one exosome at a time. The noise represents the percentage of the subtracted values of cantilevers' deflection (MBA-MD231) from the reference control values.

**Supplementary references**


1. D. J. Winchester and D. P. Winchester, *Breast Cancer*, B.C. Decker, 2006.
2. S. A. Melo, L. B. Luecke, C. Kahlert, A. F. Fernandez, S. T. Gammon, J. Kaye, V. S. LeBleu, E. A. Mittendorf, J. Weitz, N. Rahbari, C. Reissfelder, C. Pilarsky, M. F. Fraga, D. Piwnica-Worms and R. Kalluri, *Nature*, 2015, **523**, 177-182.
3. H. Im, H. Shao, Y. I. Park, V. M. Peterson, C. M. Castro, R. Weissleder and H. Lee, *Nat Biotech*, 2014, **32**, 490-495.
4. M. G. Krebs, R. L. Metcalf, L. Carter, G. Brady, F. H. Blackhall and C. Dive, *Nat Rev Clin Oncol*, 2014, **11**, 129-144.
5. G. K. Alderton, *Nat Rev Cancer*, 2015, **15**, 696-697.
6. J. Ko, E. Carpenter and D. Issadore, *Analyst*, 2016, **141**, 450-460.
7. H. Etayash and T. Thundat, in *Encyclopedia of Nanotechnology*, ed. B. Bhushan, Springer, 2015.
8. H. Etayash, K. Jiang, S. Azmi, T. Thundat and K. Kaur, *Sci Rep*, 2015, **5**, 13967.
9. T. An, S. Qin, Y. Xu, Y. Tang, Y. Huang, B. Situ, J. M. Inal and L. Zheng, *J Extracell Vesicles*, 2015.
10. G. Brock, E. Castellanos-Rizaldos, L. Hu, C. Coticchia and J. Skog, *Transl Cancer Res*, 2015, **4**, 280-290.
11. A. V. Vlassov, S. Magdaleno, R. Setterquist and R. Conrad, *Biochim Biophys Acta*, 2012, **1820**, 940-948.
12. V. Sokolova, A.-K. Ludwig, S. Hornung, O. Rotan, P. A. Horn, M. Epple and B. Giebel, *Colloids Surf Biointerfaces*, 2011, **87**, 146-150.
13. R. T. Clark, *Nat Meth*, 2015, **12**.

14. E. van der Pol, F. A. W. Coumans, A. E. Grootemaat, C. Gardiner, I. L. Sargent, P. Harrison, A. Sturk, T. G. van Leeuwen and R. Nieuwland, *J Thromb Haemost*, 2014, **12**, 1182-1192.
15. J. L. Arlett, E. B. Myers and M. L. Roukes, *Nat Nano*, 2011, **6**, 203-215.
16. J. Mertens, C. Rogero, M. Calleja, D. Ramos, J. A. Martin-Gago, C. Briones and J. Tamayo, *Nat Nanotechnol*, 2008, **3**, 301-307.
17. B. H. Cha, S. M. Lee, J. C. Park, K. S. Hwang, S. K. Kim, Y. S. Lee, B. K. Ju and T. S. Kim, *Biosens Bioelectron*, 2009, **25**, 130-135.
18. K. M. Hansen, H. F. Ji, G. Wu, R. Datar, R. Cote, A. Majumdar and T. Thundat, *Anal Chem*, 2001, **73**, 1567-1571.
19. H. Hou, X. Bai, C. Xing, B. Lu, J. Hao, X. Ke, N. Gu, B. Zhang and J. Tang, *Talanta*, 2013, **109**, 173-176.
20. W. Shu, D. Liu, M. Watari, C. K. Riener, T. Strunz, M. E. Welland, S. Balasubramanian and R. A. McKendry, *J Am Chem Soc*, 2005, **127**, 17054-17060.
21. J. Bath and A. J. Turberfield, *Nat Nanotechnol*, 2007, **2**, 275-284.
22. G. Wu, H. Ji, K. Hansen, T. Thundat, R. Datar, R. Cote, M. F. Hagan, A. K. Chakraborty and A. Majumdar, *Proc Natl Acad Sci U S A*, 2001, **98**, 1560-1564.
23. R. McKendry, J. Zhang, Y. Arntz, T. Strunz, M. Hegner, H. P. Lang, M. K. Baller, U. Certa, E. Meyer, H. J. Guntherodt and C. Gerber, *Proc Natl Acad Sci U S A*, 2002, **99**, 9783-9788.
24. T. Braun, M. K. Ghatkesar, N. Backmann, W. Grange, P. Boulanger, L. Letellier, H. P. Lang, A. Bietsch, C. Gerber and M. Hegner, *Nat Nanotechnol*, 2009, **4**, 179-185.
25. L. J. Melton, 3rd, D. M. Eddy and C. C. Johnston, Jr., *Ann Intern Med*, 1990, **112**, 516-528.
26. K. Rijal and R. Mutharasan, *Analyst*, 2013, **138**, 2943-2950.
27. D. Maraldo and R. Mutharasan, *J Food Prot*, 2007, **70**, 1670-1677.
28. G. A. Campbell and R. Mutharasan, *Environ Sci Technol*, 2007, **41**, 1668-1674.
29. Y. K. Yoo, M. S. Chae, J. Y. Kang, T. S. Kim, K. S. Hwang and J. H. Lee, *Anal Chem*, 2012, **84**, 8240-8245.
30. K. S. Hwang, M. H. Lee, J. Lee, W. S. Yeo, J. H. Lee, K. M. Kim, J. Y. Kang and T. S. Kim, *Biosens Bioelectron*, 2011, **30**, 249-254.

31. P. S. Waggoner and H. G. Craighead, *Lab Chip*, 2007, **7**, 1238-1255.
32. C. Karnati, H. Du, H. F. Ji, X. Xu, Y. Lvov, A. Mulchandani, P. Mulchandani and W. Chen, *Biosens Bioelectron*, 2007, **22**, 2636-2642.
33. M. Alvarez, A. Calle, J. Tamayo, L. M. Lechuga, A. Abad and A. Montoya, *Biosens Bioelectron*, 2003, **18**, 649-653.
34. C. Raman Suri, J. Kaur, S. Gandhi and G. S. Shekhawat, *Nanotechnology*, 2008, **19**, 235502.
35. P. J. Chapman, Z. Long, P. G. Datskos, R. Archibald and M. J. Sepaniak, *Anal Chem*, 2007, **79**, 7062-7068.
36. P. Dutta, P. J. Chapman, P. G. Datskos and M. J. Sepaniak, *Anal Chem*, 2005, **77**, 6601-6608.
37. S. Cherian, R. K. Gupta, B. C. Mullin and T. Thundat, *Biosens Bioelectron*, 2003, **19**, 411-416.
38. M. Godin, F. F. Delgado, S. Son, W. H. Grover, A. K. Bryan, A. Tzur, P. Jorgensen, K. Payer, A. D. Grossman, M. W. Kirschner and S. R. Manalis, *Nat Meth*, 2010, **7**, 387-390.
39. H. Etayash, K. Jiang, T. Thundat and K. Kaur, *Anal Chem*, 2014, **86**, 1693-1700.
40. V. Palmieri, D. Lucchetti, I. Gatto, A. Maiorana, M. Marcantoni, G. Maulucci, M. Papi, R. Pola, M. D. Spirito and A. Sgambato, *Nanoparticle Research*, 2014, **16**, 16:2583.
41. D. A. Harris, S. H. Patel, M. Gucek, A. Hendrix, W. Westbroek and J. W. Taraska, *PLoS ONE*, 2015, **10**, e0117495.